FLOW PATTERNS AND CORRESPONDING LOCAL HEAT TRANSFER COEFFICIENTS IN A PULSATING HEAT PIPE

Mauro Mameli[1], Sameer Khandekar[2], Marco Marengo[1]

[1] Department of Industrial Engineering, University of Bergamo, Viale Marconi 5, 24044 Dalmine (BG), Italy.
E-mail: marco.marengo@unibg.it ; mauro.mameli@unibg.it
[2] Department of Mechanical Engineering, Indian Institute of Technology Kanpur, 208016 Kanpur, India.
E-mail: samkhan@iitk.ac.in

ABSTRACT

A Pulsating Heat Pipe (PHP) is a passive two-phase heat transfer device for handling moderate to high heat fluxes, typically suited for power electronics and similar applications. It usually consists of a meandering capillary tube, closed end-to-end in a loop, evacuated and then partially filled with a working fluid. The internal flow patterns in a PHP are a function of the applied heat flux. At low heat flux levels, an oscillating slug flow pattern is prevalent but once the heat power increases, semi-annular and annular flow patterns gradually appear; in addition, a net fluid circulation in the entire loop may occur. In order to estimate the local heat transfer coefficient for the randomly oscillating/circulating two-phase flow, a PHP experimental apparatus has been designed and built. Relevant parameters, i.e., local fluid and wall temperatures and corresponding internal pressure fluctuations, have been recorded and the ensuing internal two-phase flow patterns have been visualized. The local heat transfer coefficient in the evaporator zone has been estimated at different heat inputs and related to the corresponding flow patterns.

INTRODUCTION

A Pulsating Heat Pipe (PHP) is not only a very promising passive heat transfer device but also a representative example of self-sustained oscillating two-phase flow in mini-channels. It usually consists of a tube, (I.D. usually between 1~3 mm, depending on the working fluid) bended in many turns, closed in an endless loop, evacuated and then partially filled with a working fluid [1,2]. Due to the capillary dimensions, the working fluid distributes itself naturally inside the tube in the form of liquid slugs and vapor bubbles (alternating slug pattern). When the evaporator section is heated, the two-phase fluid starts moving chaotically within the tube, allowing heat transfer to the condenser section by means of sensible and latent heat transfer. While the overall heat transfer performance of PHPs has been thoroughly investigated in the literature [3-8] and many qualitative trends are known, no information about the local heat transfer coefficient in the evaporator U-turns is yet available. This work is devoted to provide this local transport data vis-à-vis the internal two-phase flow patterns for an oscillating/circulating flow typically occurring in PHPs. Presented data may also be useful to fill the gaps in mini-channel flow boiling correlations and will certainly help in validating the ongoing numerical modeling of such complex systems.

EXPERIMENTAL APPARATUS AND PROCEDURE

The Pulsating heat pipe presented here consists of a closed loop with two turns (Fig. 1); the tubes in the evaporator and in the condenser sections are made of copper while the straight tubes in the adiabatic section are made of borosilicate glass for the purpose of visualization. All tubes have 4.0 mm O.D. and 2.0 mm I.D.; the distance between the evaporator and condenser ends is 250 mm. A smaller copper tube (3 mm O.D., 2 mm I.D.) has been brazed on the main tube of the condenser section in order to connect the vacuum/filling valve (make: M/s Upchurch Scientific®). A pressure transducer (make: Swagelok®, model: PTI-S-AC5-12AS) is plugged in the left external branch of the adiabatic section by mean of a T-connector (make: Swagelok®), as shown in Fig. 1.

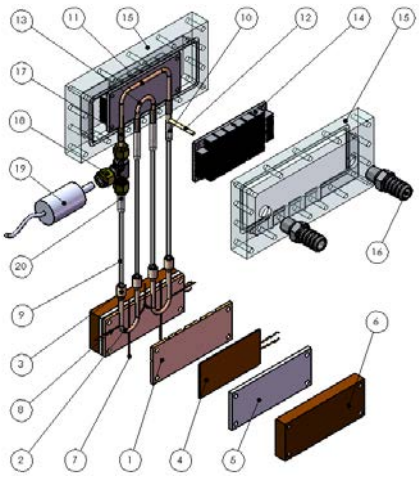

N°	ITEM
1	Evap. copper plate
2	Evap. copper U-turns
3	Copper joint
4	Heater
5	Mica sheet
6	Bakelite back plate
7	TC fluid side
8	TC wall side
9	Glass tube
10	Silicon joint
11	Condenser tube
12	Vacuum/filling tube
13	Cond. copper tube
14	Heat sink
15	Cooler shell
16	Cooling water in/out
17	Silicon seal
18	T-junction
19	Pressure transducer
20	Copper fitting

Figure 1: Test-cell assembly

The copper tubes in the condenser section are connected to the glass tubes simply by fitting a small silicon tube (5.0 mm O.D., 3.0 mm I.D.). This approach is not suitable for the copper/glass connections in the evaporator zone due to the high temperatures. In this case the following procedure has been applied:

- a copper joint is located at each end of the U-turns by mean of a steel ring and brazed;
- the glass tubes are inserted in the copper fitting and coupled to the copper tubes by mean of an O-ring;
- high temperature polymer resin (make: Omega®) fills the remaining gap between the copper fitting and the glass tube above the O-ring, thus ensuring a good seal.

The main novelty of the present work is that the two copper U-turns in the evaporator section have been drilled (1.0 mm blind hole at the top of the curvature) and two thermocouples (make: Omega®, K type, bead dimension of 0.3 mm), for measuring the fluid temperature, have been located inside the tube through the hole and fixed with thermal cement (make: Omega®), as shown in Fig. 2.

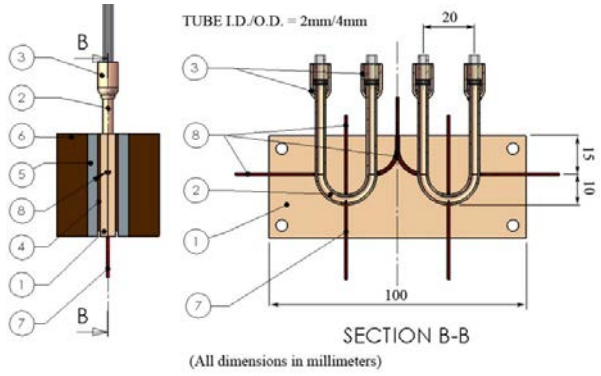

Figure 2: Test-cell, details of the evaporator zone.

Two symmetric copper plates (100 mm x 40 mm x 3 mm) have been built and circular cross section channels have been milled to embed the copper U-turns. Proper thermal contact between the U-turns and the copper plates is obtained using a high conductive paste.

Six thermocouples have been located on the external tube wall by means of small square channels milled on the copper plates. The assembly of the two plates and the U-turns forms the evaporator copper block. Two flat flexible heaters (Minco®, HR5383R10.7L12B) have been placed at each side of the evaporator block. Insulation is provided by two Mica fiber sheets (width: 3 mm) and two Bakelite® back plates (width: 12 mm). Heat input is provided by a two channel power supply (Scientific®).

The copper tubes in the condenser section are also embedded into a block with the same procedure described for the evaporator. In this case the block consists in two symmetric aluminum heat sinks which have been manufactured from a single unit. The condenser block itself fits into a custom Policarbonate shell made of two transparent plates (160 mm x 75 mm x 20 mm). Four holes allow the copper tube branches to come out the shell and connect with the adiabatic section. As shown in Fig. 3, cooling water is kept at constant temperature of 15°C ±1°C by a thermal bath and circulated through the condenser (Haake®, DC-10, K20).

All the measurement devices have been connected to a PC based data acquisition system (NI Instruments®, models: NI cDAQ9172 and NI-9211 for the thermocouples, NI USB-9162 chassis with one NI-9213 module for the pressure transducer). Sampling time for thermocouples and pressure transducer is 160 ms and 120 ms, respectively.

In order to obtain vacuum inside the PHP, a rotary gear pump (make: Varian®, model: DS102) and a turbo-molecular pump (make: Varian®, model: V-70) are connected in series to the filling valve. Filing of the PHP is only done when the internal vacuum level is at least lower than 0.01 Pa (10^{-4} mbar). In the present work all the experiments have been performed with a volumetric filling ratio of 0.65 and ethanol as the working fluid.

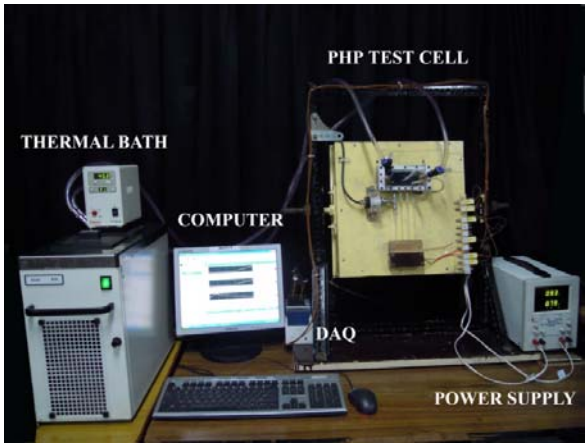

Figure 3: Experimental test-rig.

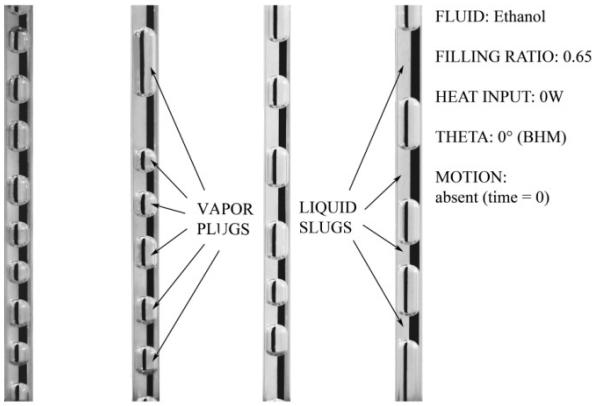

Figure 4: Steady slug flow pattern at time t = 0 sec.

A white screen with four black stripes (one for each transparent tube) has been placed behind the adiabatic section for enhancing visualization and a camera (make: Nikon®, model: Dx40) captured the different flow patterns in a 100 mm x 100 mm window just above the evaporator section; Fig. 4 shows the typical liquid slugs and vapor plug distribution just after the filling procedure.

The experimental procedure consists in vacuuming and filling the PHP at ambient temperature (25°C ± 2°C) and provide a constant heat input to the heaters. The heat input is increased with steps of 10 W as soon as the wall temperature reaches a pseudo steady state trend.

RESULTS

A series of experiments have been performed starting from different heat input levels and a common trend due to the initial heat flux has been recognized: for low initial heat input levels (from 0 to 30 W) the device behavior is mainly unstable and cannot reach a pseudo steady state even if the heat input is then increased during the experiment; for high initial heat input levels (from 40 W) the device behavior is more stable and pseudo steady state can be reached at each heat input level. For this reason, two sets of experiment have been chosen in this paper, as representatives of the two situations mentioned above.

- Experiment 1: shows the unstable behavior of the PHP for low initial start-up heat inputs (starting from 20 W);
- Experiment 2: shows that, for this simple geometry, a critical start-up heat flux is needed to commence a more stable and acceptable flow behavior that allows the estimation of the local heat transfer coefficient for each heat input level and link it with the corresponding internal two-phase flow patterns.

In all the tests, the PHP has been kept in vertical position with the evaporator zone at the bottom and the condenser at the top (Bottom Heat Mode, BHM).

Experiment 1

The wall and fluid temperature trends in the left U-turn in the evaporator section are shown in Fig. 5. Different heat input levels are also marked on the time line.

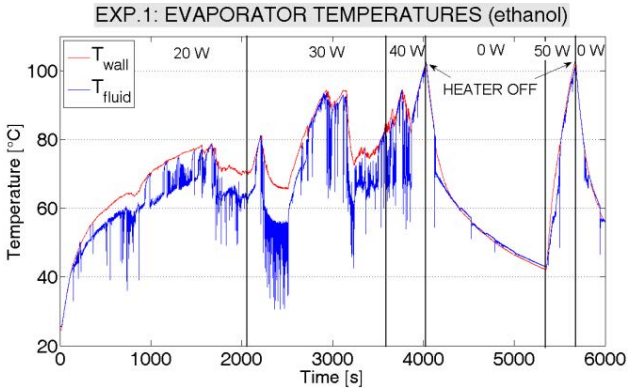

Figure 5: Experiment 1, temporal evolution of evaporator wall and fluid temperatures for different heat inputs.

It is noticeable that the fluid motion can be also identified by the oscillation of the fluid temperature; in particular, the low peaks (or troughs) are related to the passage of a cold liquid slug coming from the condenser section and the higher temperature peaks represent vapor plugs which are residing in the evaporator U-turns and being heated.

Looking closely on the first heat input period (Fig. 6), four different zones have been selected, depending on the flow motion.

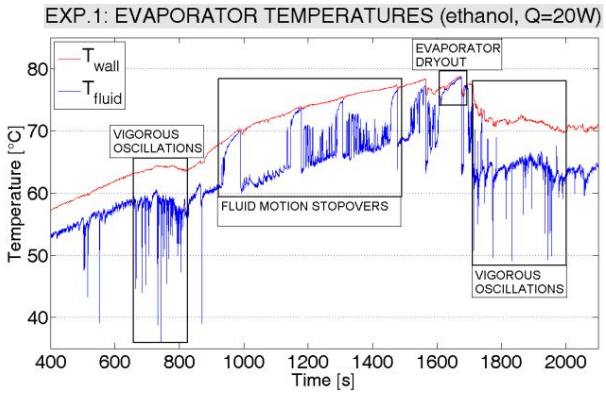

Figure 6: Experiment 1, temporal evolution of evaporator wall and fluid temperature, zoom on Q = 20W.

During the start-up (up to 700 s), the fluid motion is very poor and it is mainly due to the merging of the smaller vapor plugs; slug flow with a small oscillation amplitude is present in all branches. As soon as the local fluid temperature reaches ~ 60°C and the bigger vapor plugs approach the evaporator, fluid oscillation becomes more vigorous (first box in Fig. 6) and remains stable till the plugs and slugs distribution is unevenly distributed inside the PHP. It is evident that when the oscillation amplitude is larger, the convection is enhanced and the wall cooling is certainly more efficient.

After about 900 seconds, some big vapor plugs tend to reside/stay in the evaporator section and correspondingly big liquid slugs are seen in the condenser. This is a classic meta-stable distribution that damps the fluid oscillations: the vapor plugs residing in the evaporator are heated up and the PHP heat transfer performance is very low. If fluid temperature and pressure are still relatively low, only a small quantity of colder liquid, in the form of liquid film draining from the hanging menisci, is able to reach the evaporator and only a small fluid pulsation is restored. If the slug and plug distribution is again balanced, this stopover phenomenon repeats (second box in Fig. 6) and both wall and fluid temperature keep on rising because of the low heat transfer rate.

If the fluid temperature goes beyond a threshold (between 70 and 75°C) and fluid motion is still poor, all the liquid film surrounding the vapor plugs evaporates and dry-out occurs (third box in Fig. 6) and the fluid temperature reaches the wall temperature. At this point many different scenarios may occur. At low heat input levels, flow instability may restore an uneven plug and slug distribution and also more vigorous oscillations (forth box in Fig. 6).

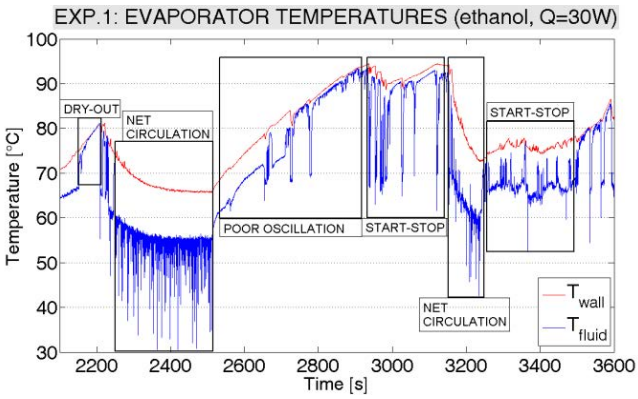

Figure 7: Experiment 1, temporal evolution of evaporator wall and fluid temperature, zoom on Q = 30 W.

At this stage, raising the heat input level to 30 W does not improve the behavior and may lead to a new dry-out (first box in Fig. 7). More so, such a condition may also evolve abruptly in a new flow motion characterized by a net circulation (never present for lower heat inputs) which shows the best efficiency (second box in Fig. 7). When the fluid and wall temperatures decrease, also the fluid pressure decreases and the net circulation of the fluid cannot be supported anymore. The device starts working as a sort of a heat switch: fluid temperature and pressure rise when fluid oscillations are poor and again decrease, when more vigorous flow motion is activated. Sometimes, as shown in Fig. 8, dry-outs may not evolve at all, at 40 W the poor fluid motion leads to a faster temperature increase and to a consolidation of the inefficient slug and plug position. The power supply has been switched off and again switched on at 50 W but the previous even distribution lead to another fast dry-out.

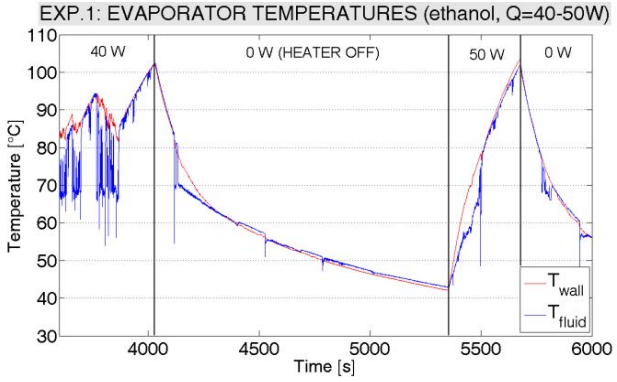

Figure 8: Experiment 1, temporal evolution of evaporator wall and fluid temperature, zoom on Q = 40-50W.

The impossibility of getting a steady-state and therefore an acceptable stable thermal performance is mainly due to the simple geometry of the present test-rig. It has been documented by Charoensawan et al. [9] that this unstable behavior can be mitigated, or even eliminated, by increasing the number of U-turns. By doing this, the number of heated and cooled section, as well as the local pressure fluctuations due to bends and turns also increase. This leads to an intrinsic higher probability of liquid slug break-ups and uneven distribution of plugs and slugs, which indeed is the desired pre-requisite of stable thermal performance of a PHP.

Experiment 2

The solution for the present test rig, where geometry could not be changed, is to increase the initial heat input level to 40W as shown in Fig. 9.

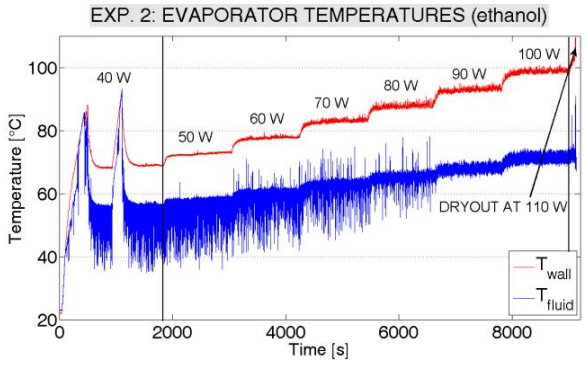

Figure 9: Experiment 2, temporal evolution of evaporator wall and fluid temperatures for different heat inputs.

For this experimental apparatus it seems that a critical initial heat flux $q'' = \dot{Q} / A_{ev}$ = 5.2 - 6.5 W/m^2, where $\dot{Q}$ is the heat input level and $A_{ev} = \pi \cdot d_{in} \cdot L_{ev}[m^2]$ is the internal evaporator tube area, is mandatory in order to sustain a stable condition right from the start. Indeed, even if at 40W (q" = 5.2 W/cm^2) the device still operates in the 'Heat Switch Mode' described for experiment 1, from 50 W to 100 W (q" = 6.5 to 13.0 W/cm^2) the net circulating flow is definitely dominant in the PHP without any unstable events, as noted in Experiment 1.
In order to show that the net fluid circulation is always accompanied by oscillation, the fluid pressure signal over time has been plotted in Fig. 10. The amplitude of the fluid pressure oscillation increases with the heat input level.

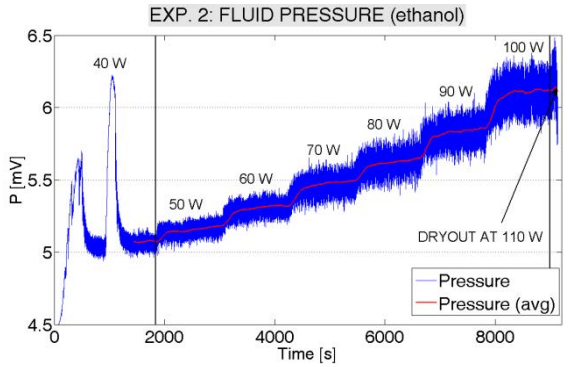

Figure 10: Experiment 2, temporal evolution of local fluid pressure signal for different heat inputs.

Another clear observation is that during the second pressure ramp, which obviously corresponds to the local dry-out in Fig. 9, there are no oscillations; the corresponding absence of fluid motion is also confirmed by visualization (Fig. 11).

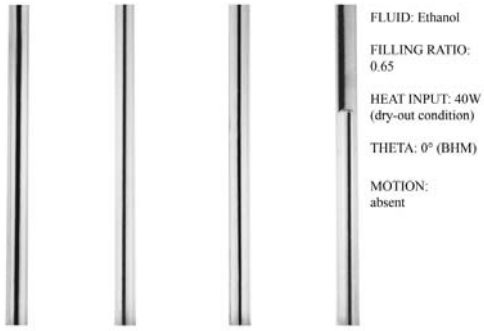

Figure 11: Experiment 2, local dry-out during the start-up.

During Experiment 2 a pseudo steady state occur at each heat input level and this is a necessary condition for the local heat transfer coefficient calculation:

$$\tilde{h}_{ev} = \frac{\dot{Q}}{\Delta T_{w-f} * A_{ev}} [W / m^2 K] \quad (1)$$

where, ΔT_{w-f} is the difference between the wall and fluid temperatures, plotted in Fig. 9. The local heat transfer coefficient in the evaporator zone (blue line) and its moving average (red line) are shown in Fig. 12. The plot also corresponds to the five different flow patterns which have been recognized during the PHP operation and captured by the camera.

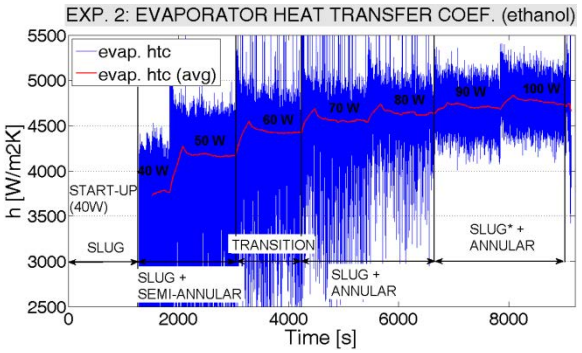

Figure 12: Experiment 2, temporal evolution of local heat transfer coefficient and flow regimes for different heat inputs.

Before describing all the flow patterns and the related local heat transfer coefficients it is worthwhile to show a representative picture of the start-up period (Fig. 13). The flow pattern is completely slug in all the four branches and the flow motion is mainly oscillating. As mentioned for Experiment 1, this stage is characterized by merging of the smaller vapor plugs and formation of bigger ones.

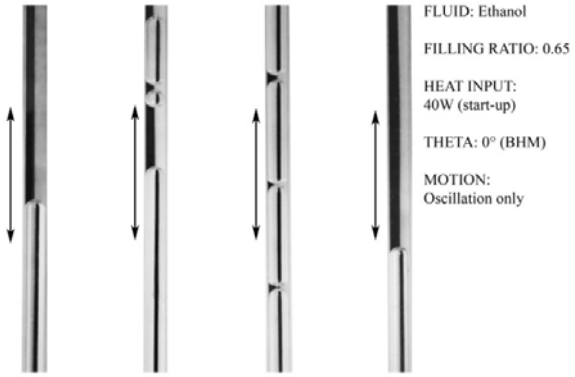

Figure 13: Experiment 2, flow pattern during the start-up period (SLUG FLOW).

When the heat input level is between 40 W and 50 W, net flow circulation becomes a constant feature. If a vapor plug coming from the a slug flow down-comer is passing through the heated section (i.e., left evaporator U-turn), a part of its liquid film evaporates into the vapor plugs and the resulting vapor pressure becomes strong enough to push the adjacent liquid slug through the next branch up to the condenser section. This is exactly what is happening in the second branch of Fig. 14, where a liquid slug is being pushed against gravity by the vapour expansion occurring in the left evaporator U-turn.
Due to symmetry, the same phenomena are also happening in the third and fourth branches and, since the device is closed in a loop, the vapour pressure in the last branch pushes the fluid up to the condenser and then again down in the first branch (flow direction is explicitly shown in Fig. 14).

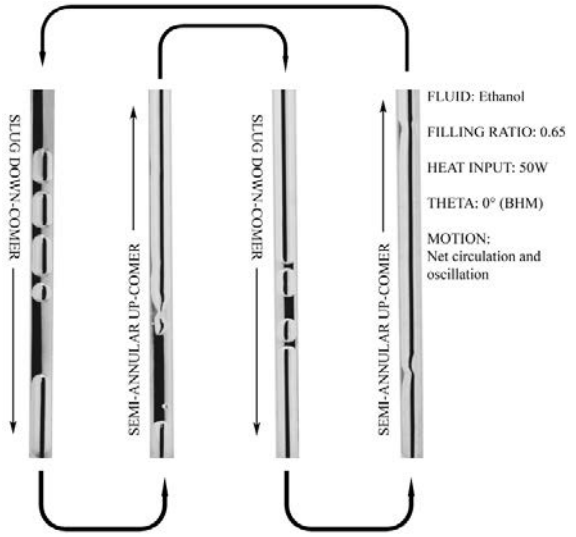

Figure 14: Experiment 2, flow pattern during the pseudo steady state at 40-50W (SLUG + SEMI-ANNULAR).

Thus, owing to a well defined flow circulation, a conspicuous amount of liquid, may be in the form of liquid slugs or in the form of a thin liquid film surrounding each vapour plug, is always available in the evaporator section. Regarding the flow pattern, the first and third branches are always pure slug down-comer and the second and fourth branches are characterized by a semi-annular flow pattern, consisting of long annular periods alternated with some occasional transits of the liquid slugs.

When the heat input level goes up to 60 W (Fig. 15) a flow pattern transition occurs in the two up-comers.

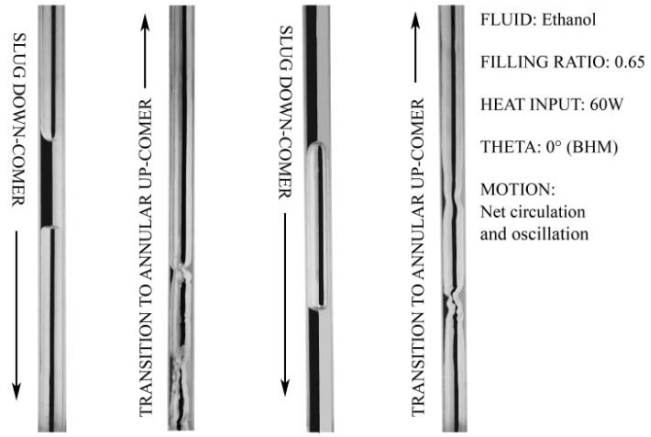

Figure 15: Experiment 2, flow pattern during the pseudo steady state at 60W (TRANSITION from semi-annular to annular up-comers).

The vapour pressure, and the resulting inertia force thereof, in the evaporator section, is now able to break most of the liquid slug menisci bridges and therefore the flow pattern in the two up-comers is changing from semi-annular to pure annular. The liquid film is thick and wavy and a higher amount of the heat transfer is due to the latent heat of vaporization; a 6% gain of the local heat transfer coefficient is recorded with respect to the previous heat input level.

When the heat input level is augmented to 70 W (Fig. 16) and then to 80 W the fluid, which is going up through the second and third branch, has reached the fully annular flow pattern. The liquid film is thinner and less surface waviness is recorded. The local heat transfer coefficient growth is pretty much lower with respect to the previous case (respectively 3.4% and 2.2%) confirming the fact that most of the local heat transfer is due to latent heat and the system is about to reach its maximum potential.

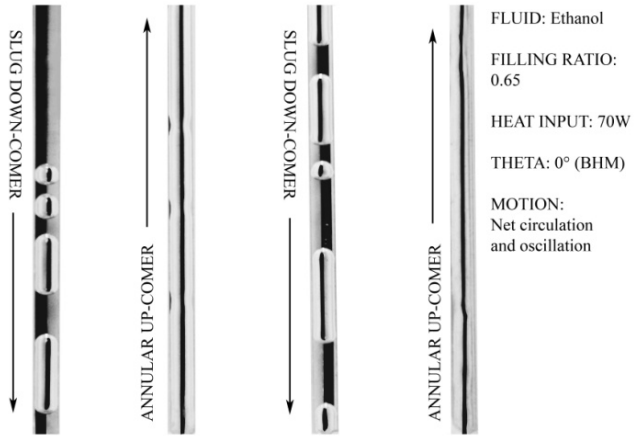

Figure 16: Experiment 2, flow pattern during the pseudo steady state at 70W (SLUG + ANNULAR).

Finally, the last two stable pseudo steady states (90 W and 100 W) are again characterized by annular up-comers and slug-flow down-comers. In these cases, the liquid film in the two up-comers is very thin and, in spite the pressure signal is widely oscillating (liquid slugs in the third down-comer are getting deformed by the strong oscillation), the fluid temperature in the evaporator is not having large variations as before: the high heat power is now able to evaporate the great majority of the liquid coming from the slug down-comer without any vapor reflux.

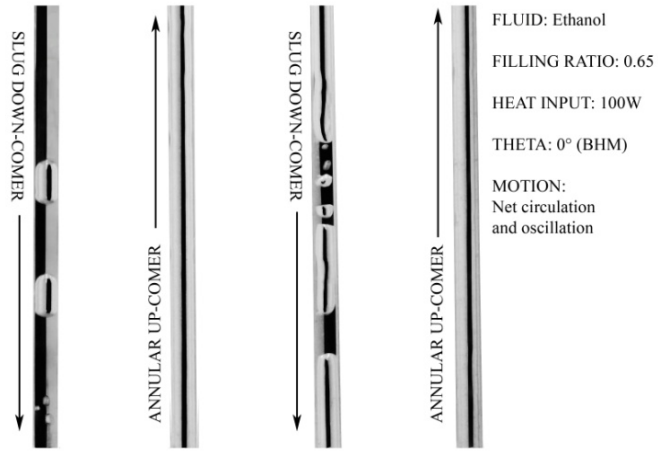

Figure 17: Experiment 2, flow pattern during the pseudo steady state at 100W (SLUG (*unstable film thickness) + ANNULAR).

The local heat transfer coefficient is now coming to an asymptotic value and the gain with respect to the previous cases is only around 1%. If the heat input level is increased to 110 W, the slug down-comers are not able to provide a sufficient amount of fresh liquid phase and an abrupt dry-out occurs in a few minutes.

In order to appreciate the overall performance of such device, the overall thermal conductivity (Fig. 18) has been calculated as follows:

$$k_{eq} = \frac{\dot{Q}}{A_{cr}} \frac{L_{tot}}{\Delta T_{w-c}} \tag{2}$$

where, $A_{cr} = n \cdot \pi \cdot {d_{out}}^2 / 4$ is the total radial PHP cross section area, L_{tot} is the distance between the hot source and the cooling one and ΔT_{w-c} is the difference between the wall temperature (hot side) and the average temperature of the cooling water in the condenser zone (cold side).

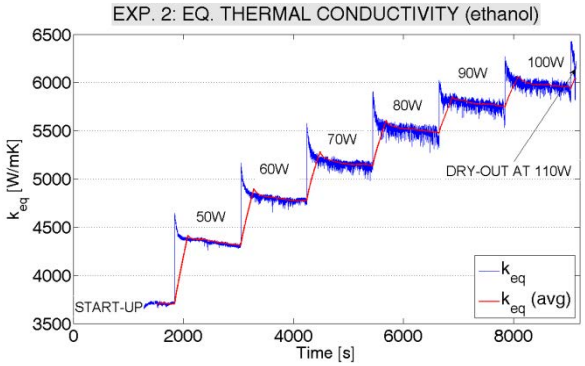

Figure 18: Experiment 2, equivalent thermal conductivity over time for each heat input level.

This value can be easily compared with the thermal conductivity of the substrate material by defining a enhancement factor EF= k_{eq}/ k_s and also with the values extrapolated from other test-rigs in literature (Tab. 1).

Tab.1: Equivalent thermal conductivity and enhancement factors for different PHPs.

Author	material / support	L_{tot} [m]	n [-]	A_{cr} [m^2]	$\dot{Q}_{max}$ [W]	ΔT_{w-c} [K]	k_eq [W/m.K]	EF [-]
Akachi [2]	copper / tube d_{out} = 3mm	0,46	160	0,00113	2000	90	9038	22,6
Yang et al. [10]	copper / tube d_{out} = 3mm	0,12	40	0,00028	400	123	1380	3,4
Yang et al. [11]	aluminium / plate	0,18	66	0,00036	400	75	2666	10,6
Lin et al. [12]	PDMS / plate	0,06	12	0,00112	8	80	5	29,0
Mameli et al.	copper / tube d_{out} = 4mm	0,2	4	5e-5	100	84	5920	14,8

In spite of its simple geometry the present PHP shows an appealing performance. When a net circulation occurs, the overall thermal conductivity is comprised between 4310 W/mK and 5920 W/mK which means that the device is working from 10 to 14 times better than pure copper.

CONCLUSIONS

A novel PHP experimental apparatus has been designed in order to record both local fluid and wall temperatures in the evaporator zone, acquire the pressure signal and capture the slugs and plugs distribution in the adiabatic zone. The following conclusions can be drawn:

- When the number of turns is small a critical heat flux between 5.2 and 6.5 W/cm2 is needed to ignite a stable fluid motion and reach an acceptable pseudo steady state.
- When a stable steady state is reached, a net circulation, together with an oscillating component, is always recognizable at each heat input level.
- The local heat transfer coefficient in the evaporator zone has been calculated and related to the different flow patterns which have been visualized at each heat input level. $\tilde{h}_{ev}$ approaches an asymptotic value around 4600W/m^2K, before the final dry-out occurs.
- Even though the present PHP has a very simple geometry (only two turns), its overall effective thermal conductivity can reach 5920W/mK which is an appealing value for practical applications.
- Further research should be devoted to the slug plug distribution control in order that PHPs with a small number of turns can also reliably work in a wider range of boundary conditions.

NOMENCLATURE

Symbol	Quantity	SI Unit
A	Surface area	m^2
d	Diameter	m
$\tilde{h}$	Local heat transfer coefficient	W/ m^2K
k	Thermal conductivity	W/mK
L	Length	m
n	Number of parallel channels	[-]
q”	Heat flux	W/cm^2
$\dot{Q}$	Power heat input	W
T	Temperature	°C

Subscrtipts

cr	Cross section
ev	Evaporator
eq	Equivalent
fluid	Fluid
in	Inner
max	Maximum
out	Outer
tot	Total
wall	Wall
w-f	Wall to working fluid
w-c	Wall to cooling medium

REFERENCES

[1] Akachi, H. Structure of a Heat Pipe. U.S. Patent Number 4921041 (1990).

[2] Akachi, H. Structure of Micro-Heat Pipe. U.S. Patent Number 5219020 (1993).

[3] Khandekar S., Charoensawan P., and Groll M., and Terdtoon P., Closed Loop Pulsating Heat Pipes-Part B: Visualization and Semi-Empirical Modeling, App. Therm. Eng., Vol. 23(16), pp. 2021-2033, 2003.

[4] Kim J. S., Bui N. H., Kim J. H., Kim J. W., and Jung H. S. Flow Visualization of Oscillation Characteristics of Liquid and Vapor Flow in the Oscillating Capillary Tube Heat Pipe KSME Int. J., Vol. 17(10), pp. 1507-1519, 2003.

[5] Khandekar S. and Groll M., An Insight into Thermo-Hydraulic Coupling in Pulsating Heat Pipes, Int. J. of Thermal Sciences, Vol. 43(1), pp. 13-20, 2004.

[6] Liu S., Li J., Dong X., and Chen H., Experimental Study of Flow Patterns and Improved Configurations for Pulsating Heat Pipes, Int. J. of Thermal Science, Vol. 16(1), pp. 56-62, 2007.

[7] Intagun W., Sakulchangsatjatai P., and Terdtoon P., Effect of Working Fluids on Internal Flow Patterns of Closed - Loop Oscillating Heat Pipe at Maximum Heat Flux State, Proc. 9th Int. Heat Pipe Symp., Kuala Lumpur, Malaysia, 2008.

[8] Khandekar S., Gautam A. P. and Sharma P., Multiple Quasi-Steady States in a Closed Loop Pulsating Heat Pipe, Int. J. of Thermal Sciences, Vol. 48(3), pp. 535-546, 2009.

[9] Charoensawan, P., and Terdtoon, P., Thermal Performance of Horizontal Closed-loop Pulsating Heat Pipes. App. Therm. Eng., Vol. 28, pp. 460-466, 2008.

[10] Yang H., Khandekar S., and Groll M., Operational Limit of Closed Loop Pulsating Heat Pipes, App. Therm. Eng., Vol. 28, pp. 49-59, 2008.

[11] Yang H., Khandekar S., and Groll M., Performance Characteristics of Pulsating Heat Pipes as Integral Thermal Spreaders, Int. J. of Thermal Sciences, Vol. 48, pp. 815-824, 2009.

[12] Lin Y.H., Kang S.H., Wu T.Y., Fabrication of Polydimethyl - siloxane (PDMS) Pulsating Heat Pipe, App. Therm. Eng., Vol. 29, pp. 573-580, 2009.